Geophysical Prospecting, 1980, 28, 146–166.

FINITE-DIFFERENCE EVALUATION OF APPARENT RESISTIVITY CURVES*

I.R. MUFTI**

ABSTRACT

MUFTI I.R. 1980, Finite-Difference Evaluation of Restivity Curves, Geophysical Prospecting 28, 146–166.

The problem of numerical evaluation of apparent resistivity curves is treated by finite difference modeling. The models proposed are set up in cylindrical coordinates and yield the potential field due to a point source located in a radially symmetric environment. The Schlumberger configuration, widely used for surface measurements, is emphasized. However, the treatment is equally applicable to other similar situations such as the computation of synthetic electric logs when the resistivity of the borehole fluid is different from that of the surrounding uniform or stratified medium. Moreover, the individual layers may not necessarily be isotropic.

The medium under investigation is discretized by using a very coarse system of horizontal and vertical grid lines whose distance from the source increases logarithmically; consequently, the physical dimensions of the medium can be made "infinite" without affecting the numerical size of the model. Finer features such as a thin but anomalously resistive or conductive bed which would ordinarily be missed in coarse discretization are accurately taken into account, since the calculations are done in terms of the Dar Zarrouk parameters derived from the exact resistivity distribution of the model. This enables one to compute the potential field by inverting a small sparse matrix. When the medium comprises only a few layers, the efficiency of the finite-difference model is comparable to that of the known analytical methods; for more complicated structures, however, the finite-difference model becomes more efficient. The accuracy of finite-difference results is demonstrated by comparing them with the corresponding analytically obtained data.

1. INTRODUCTION

The problem of numerical evaluation of apparent resistivity curves has attracted the attention of theoreticians ever since the birth of the resistivity method (Hummel 1932, Tagg 1932). A comprehensive investigation of this problem was attempted by Stefanesco, C. Schlumberger and M. Schlumberger

* Received December 1977.

** Amoco Production Company, Research Center, Tulsa, Oklahoma, USA.

0016-8025/80/0200-0146 $02.00

(1930); although their theoretical treatment is valid for any number of layers, the progress in numerical evaluation has been possible only in small steps (Flathe 1955, van Dam 1965, Mooney, Orellana, Pickett and Tornheim 1966, Argelo 1967, Koefoed 1968, Deppermann 1973). During the same period, several sets of precomputed master curves became available (Mooney and Wetzel 1956, CGG 1963, Anonymous 1963a, b, Orellana and Mooney 1966, EAEG 1969). All these sets of curves have played a valuable role, but none of them offers a sufficient variety of curves needed for the interpretation of field data. Borm (1972, 1973) attempted to evaluate apparent resistivity curves by means of analog models. Unfortunately, such models are very cumbersome to set up and yield results that are significantly less accurate than those obtained by analytical means. Recently an alternative scheme based on the evaluation of a resistivity transform function of the raised kernel function was introduced by Ghosh (1971a, b). By demonstrating a linear relationship between the apparent resistivity and the resistivity transform function, he introduced a method which is computationally quite efficient.

We shall describe below a very simple finite-difference algorithm for the evaluation of apparent resistivity curves for a parallel-layer earth; it is both fast and accurate and computes the potential field due to a point source.

It is a well-known fact that by increasing the number of grid points a finite-difference model can be made extremely accurate; but, since this leads to increasing computer costs, it is not a practical approach. This remark particularly applies to the resistivity problem, because the presence of a point source implies the necessity of setting up a three-dimensional model. We shall overcome this difficulty by:

1. Introducing nonuniform grid spacing for discretizing the medium,
2. Setting up the model in cylindrical coordinates and assuming radial symmetry,
3. Replacing complex multilayered structures by the electrically equivalent but locally uniform structures. This will be accomplished by making use of the Dar Zarrouk parameters first introduced by Maillet (1947).

2. Resistivity Models with Radial Symmetry

The fundamental relation governing the flow of steady electric current in a nonuniform medium is given by

$$\nabla \cdot \left[\frac{1}{\rho(x, y, z)} \nabla v(x, y, z) \right] + q(x, y, z) = 0 \tag{1}$$

where ρ is the resistivity of the medium [Ω m], v the potential [volt], and q the strength of the current source [A m^{-3}].

If we use cylindrical coordinates and assume radial symmetry, (1) can be expressed as:

$$\frac{1}{r}\frac{\partial}{\partial r}\left[\frac{1}{\rho(r,z)}r\frac{\partial v(r,z)}{\partial r}\right]+\frac{\partial}{\partial z}\left[\frac{1}{\rho(r,z)}\frac{\partial v(r,z)}{\partial z}\right]+q(r,z)=0. \tag{2}$$

It is convenient to substitute

$$1/\rho(r,z)=\sigma(r,z)$$

and rewrite (2) in the self-adjoint form

$$\frac{\partial}{\partial r}\left[\sigma(r,z)\frac{\partial v(r,z)}{\partial r}\right]+\frac{\partial}{\partial z}\left[\sigma(r,z)\frac{\partial v(r,z)}{\partial z}\right]+\frac{1}{r}\sigma(r,z)\frac{\partial v(r,z)}{\partial r}+q(r,z)=0, \qquad r>0. \tag{3}$$

We shall use (3) for evaluating the potential field due to a point source located at the surface or inside the ground. Note that the third term on the left-hand side of (3) involves division by r; it will pose problems in the numerical evaluation of the potential along the vertical axis $r=0$. This difficulty can be avoided by making use of the fact that

$$\lim_{r\to 0}\frac{1}{r}\frac{\partial v(r,z)}{\partial r}=\left[\frac{\partial^2 v(r,z)}{\partial r^2}\right]_{r=0}. \tag{4}$$

Therefore, for evaluating the potential along the axis of symmetry, (3) must be replaced by:

$$\frac{\partial}{\partial r}\left[\sigma(r,z)\frac{\partial v(r,z)}{\partial r}\right]+\frac{\partial}{\partial z}\left[\sigma(r,z)\frac{\partial v(r,z)}{\partial z}\right]+\sigma(r,z)\frac{\partial^2 v(r,z)}{\partial r^2}+q(r,z)=0 \qquad r=0. \tag{5}$$

When we are dealing with an anisotropic medium, (3) takes the form

$$\frac{\partial}{\partial r}\left[\sigma_{\parallel}(r,z)\frac{\partial v(r,z)}{\partial r}\right]+\frac{\partial}{\partial z}\left[\sigma_{\perp}(r,z)\frac{\partial v(r,z)}{\partial z}\right]+\frac{1}{r}\sigma_{\parallel}(r,z)\frac{\partial v(r,z)}{\partial r}+q(r,z)=0, \tag{6}$$

where

$$\sigma_{\parallel}/\sigma_{\perp}=\lambda. \tag{7}$$

$\sigma_{\parallel}$ and $\sigma_{\perp}$, respectively, denote conductivity of the medium parallel and

perpendicular to the direction of stratification and λ is called the coefficient of anisotropy (Bhattacharya and Patra 1968). On the other hand, when the medium consists of a system of homogeneous and isotropic horizontal layers, σ varies only with z, and (3) and (5) reduce to

$$\sigma(z)\left[\frac{\partial^2 v(r, z)}{\partial r^2} + \frac{1}{r}\frac{\partial v(r, z)}{\partial r}\right] + \frac{\partial}{\partial z}\left[\sigma(z)\frac{\partial v(r, z)}{\partial z}\right] + q(r, z) = 0, \qquad r > 0. \quad (8)$$

$$2\sigma(z)\frac{\partial^2 v(r, z)}{\partial r^2} + \frac{\partial}{\partial z}\left[\sigma(z)\frac{\partial v(r, z)}{\partial z}\right] + q(r, z) = 0, \qquad r = 0. \quad (9)$$

The rest of the treatment will be primarily devoted to the evaluation of apparent resistivity curves by assuming a point source dipole and Schlumberger configuration over a horizontally stratified medium. However, the treatment is quite general and is equally applicable to all other situations involving radial symmetry. Thus, it could be used for computing synthetic electric logs due to a point source moving along a borehole filled with a drilling fluid whose resistivity is different from that of the surrounding uniform or stratified medium.

Fig. 1 represents a vertical section through the ground. For a finite-difference model, we consider only a finite portion of the semi-infinite

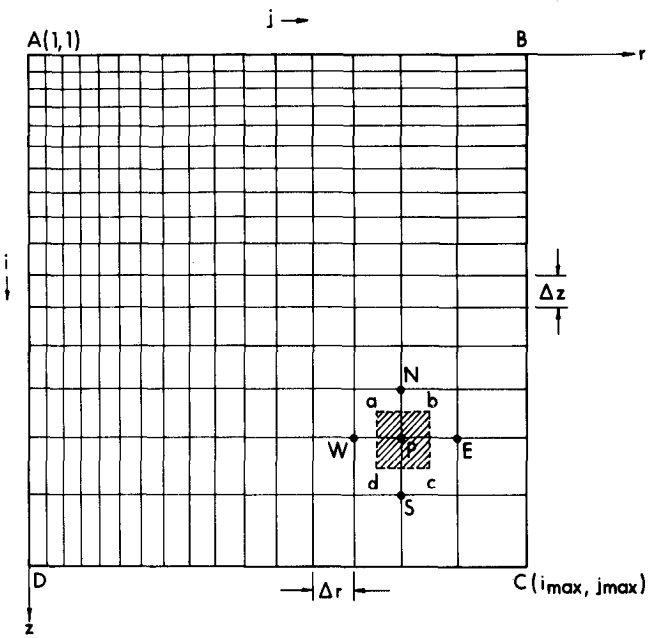

Fig. 1. Example of a finite-difference model in cylindrical coordinates with expanding grid system.

medium; it is enclosed by the boundary *ABCDA*. Since the field is symmetrical around the *z*-axis, the figure shows only one-half of the model. Let us divide the area enclosed by *ABCDA* into a number of rectangular cells and replace each cell by a point. Thus, the point *P* represents the rectangular area *abcd* of the vertical section of the subsurface. We shall call each of these points an element of the model. An element corresponding to the *i*th row and the *j*th column will be denoted by (i, j), its location expressed in cylindrical coordinates will be

$$r = \sum_{k=2}^{j} \Delta r(k-1, k); \qquad z = \sum_{l=2}^{i} \Delta z(l-1, l), \tag{10}$$

where $\Delta r(k-1, k)$ denotes the spacing between the columns $k-1$ and k, and $\Delta z(l-1, l)$ is the spacing between the rows $l-1$ and l of the model. $j = 1$ corresponds to the vertical axis ($r = 0$) and $i = 1$ denotes the surface of the ground ($z = 0$). $j = j_{max}$ and $i = i_{max}$, respectively, denote the boundaries *BC* and *CD*. By successively increasing the intervals Δr and Δz as we recede from the source located at (1, 1), we can consider an arbitrarily large volume of the earth without enormously increasing the computational size of the model.

Let the set of elements (i, j) located inside the boundary *ABCDA* be denoted by *G*. We want to compute the potential for $(i, j) \in G$ due to a current source located at (1, 1) of strength *I* A, subject to the following boundary conditions

$$\frac{\partial v}{\partial z} = 0, \{(i, j) | i = 1, j = 1, \ldots j_{max}\}, \tag{11}$$

$$\frac{\partial v}{\partial r} = 0, \{(i, j) | j = 1, i = 1, \ldots (i_{max} - 1)\}, \tag{12}$$

$$v = 0, \begin{matrix} |\{(i, j) | j = j_{max}, i = 2, \ldots i_{max}\} \\ |\{(i, j) | i = i_{max}, j = 2, \ldots j_{max}\} \end{matrix}. \tag{13}$$

Condition (11) ensures that there is no flow of current across the surface of the ground, whereas condition (12) is introduced on account of radial symmetry. Conditions (13) imply that the influence of the source at the boundaries *BC* and *CD* becomes negligible.

3. Derivation of Finite-Difference Equations

To start with, we shall consider the elements $(i, j) \in G$. One such element *P* and its four immediate neighbors *E*, *N*, *W*, and *S* are shown in fig. 2. Let the distances of *P* from *E*, *N*, *W*, and *S* be denoted by h_E, h_N, h_W, and h_S. A

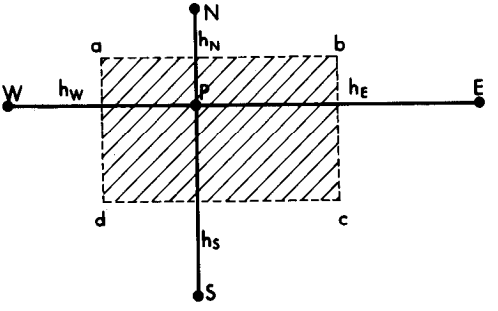

Fig. 2. An arbitrarily chosen element P of the finite-difference model with its four immediate neighbours E, N, W, and S.

finite-difference equation which relates the potential at P to the potentials at E, N, W, and S can be derived from (3) by the application of the central difference formula (see, for example, Young 1962). Thus, the first term on the left-hand side of (3) leads to

$$\frac{\partial}{\partial r}\left(\sigma\frac{\partial v}{\partial r}\right)_{ij} = \frac{2}{h_E + h_W}\left[\left(\sigma\frac{\partial v}{\partial r}\right)_{i,\,j+h_E/2} - \left(\sigma\frac{\partial v}{\partial r}\right)_{i,\,j-h_W/2}\right]$$

$$= \frac{2}{h_E + h_W}\left[\frac{\sigma_{i,\,j+h_E/2}}{h_E}\left(v_{i,\,j+h_E} - v_{i,\,j}\right) - \frac{\sigma_{i,\,j-h_W/2}}{h_W}\left(v_{i,\,j} - v_{i,\,j-h_W}\right)\right], \tag{14}$$

where

$$\left.\begin{aligned} &\sigma_{i,\,j+h_E/2} = (\sigma_{i,\,j} + \sigma_{i,\,j+h_E})/2 \\ &\text{and} \\ &\sigma_{i,\,j-h_W/2} = (\sigma_{i,\,j} + \sigma_{i,\,j-h_W})/2 \end{aligned}\right\} \tag{15}$$

denote the values of conductivity at $(i, j + h_E/2)$ and $(i, j - h_W/2)$, respectively. Proceeding like that, the finite-difference equivalent of (3) can be obtained in the form

$$\frac{2}{h_E + h_W}\left[\frac{\sigma_{i,\,j+h_E/2}}{h_E}\left(v_{i,\,j+h_E} - v_{i,\,j}\right) - \frac{\sigma_{i,\,j-h_W/2}}{h_W}\left(v_{i,\,j} - v_{i,\,j-h_W}\right)\right]$$

$$+ \frac{2}{h_N + h_S}\left[\frac{\sigma_{i+h_S/2,\,j}}{h_S}\left(v_{i+h_{S,j}} - v_{i,\,j}\right) - \frac{\sigma_{i-h_N/2,\,j}}{h_N}\left(v_{i,\,j} - v_{i-h_N,\,j}\right)\right]$$

$$+ \frac{\sigma_{i,\,j}}{r(h_E + h_W)}\left(v_{i,\,j+h_E} - v_{i,\,j-h_W}\right) + q_{i,\,j} = 0, \tag{16}$$

where r is given by (10).

A finite-difference equation similar to (16) but derived for two-dimensional structures is given by Mufti (1976). In order to gain a better insight into the physical aspect of the problem, let us introduce a slight modification. The area of the hatched zone associated with the element P (fig. 2) is given by

$$\left(\frac{h_E + h_W}{2}\right)\left(\frac{h_N + h_S}{2}\right). \tag{17}$$

If we multiply (16) throughout by (17), we get

$$\alpha_E(i, j)v_{i, j+h_E} + \alpha_N(i, j)v_{i-h_N, j} + \alpha_W(i, j)v_{i, j-h_W} + \alpha_S(i, j)v_{i+h_S, j} - \alpha_P(i, j)v_{i, j} + \tilde{q}_{i, j} = 0, \qquad (i, j) \in G, \tag{18}$$

where

$$\alpha_E(i, j) = \sigma_{i, j+h_E/2}\left(\frac{1}{h_E} + \frac{1}{2r}\right)\left(\frac{h_N + h_S}{2}\right), \tag{19}$$

$$\alpha_W(i, j) = \sigma_{i, j-h_W/2}\left(\frac{1}{h_W} - \frac{1}{2r}\right)\left(\frac{h_N + h_S}{2}\right), \tag{20}$$

$$\alpha_N(i, j) = \sigma_{i-h_N/2, j}\left(\frac{1}{h_N}\right)\left(\frac{h_E + h_W}{2}\right), \tag{21}$$

$$\alpha_S(i, j) = \sigma_{i+h_S/2, j}\left(\frac{1}{h_S}\right)\left(\frac{h_E + h_W}{2}\right), \tag{22}$$

$$\alpha_P(i, j) = \alpha_E(i, j) + \alpha_W(i, j) + \alpha_N(i, j) + \alpha_S(i, j), \tag{23}$$

$$\tilde{q}_{i, j} = q_{i, j}\left(\frac{h_E + h_W}{2}\right)\left(\frac{h_N + h_S}{2}\right). \tag{24}$$

Since $q_{i, j}$ means the current density and the element P represents the area (17), $\tilde{q}_{i, j}$ denotes the current entering the medium at P. If P corresponds to a negative current electrode, $\tilde{q}_{i, j}$ should be replaced by $-\tilde{q}_{i, j}$; when it corresponds to a potential electrode, $\tilde{q}_{i, j} = 0$.

The set of coefficients given by (19)–(23) will be referred to as the conductivity coefficients; they are valid only for the elements inside the boundaries of the model. We shall now consider the elements along the various boundaries starting with the surface boundary.

The coefficients for the set of elements $\{(i, j) \mid i = 1\}$ must be computed subject to condition (11). This can be done by introducing a fictitious row of elements $\{(i, j) \mid i = 0\}$ such that

$$\Delta z(0, 1) = \Delta z(1, 2), \tag{25}$$

$$\left.\begin{aligned}\sigma_{0,j} &= \sigma_{2,j}\\ v_{0,j} &= v_{2,j}\end{aligned}\right\} j = 1, \ldots, \quad j_{max}. \tag{26}$$

(27)

On account of (25) and (26), we have

$$\alpha_N(1,j) = \alpha_S(1,j), \qquad j = 1, \ldots, j_{max}. \tag{28}$$

Since the evaluation of $\alpha_N(1,j)$ requires fictitious data $\sigma_{0,j}$ and $\Delta z(0,1)$, we use (28) to eliminate $\alpha_N(1,j)$ from (18). This leads to

$$\alpha_E(1,j)v_{1,j+h_E} + \alpha_W(1,j)v_{1,j-h_W} + 2\alpha_S(1,j)v_{1+h_S,j} - \alpha_P(1,j)v_{1,j} + \tilde{q}_{1,j} = 0, \qquad j = 2, 3, \ldots, (j_{max}-1). \tag{29}$$

For automatic computations in a digital computer, it would be more efficient to treat (29) as a special case of (18). This can be done by retaining $\alpha_N(i,j)$, but setting it equal to zero. Moreover, in view of (26), $h_N = h_S$. Consequently, for $i = 1$, the coefficients appearing in (18) will be given by:

$$\alpha_E(1,j) = \sigma_{1,j+h_E/2}\left(\frac{1}{h_E} + \frac{1}{2r}\right)h_S, \tag{30}$$

$$\alpha_W(1,j) = \sigma_{1,j-h_W/2}\left(\frac{1}{h_W} - \frac{1}{2r}\right)h_S, \tag{31}$$

$$\alpha_N(1,j) = 0, \qquad j = 2, \ldots, (j_{mx}-1) \tag{32}$$

$$\alpha_S(1,j) = 2\sigma_{1+h_S/2,j}\left(\frac{1}{h_S}\right)\left(\frac{h_E+h_W}{2}\right), \tag{33}$$

$$\tilde{q}_{1,j} = q_{1,j}\left(\frac{h_E+h_W}{2}\right)h_S. \tag{34}$$

We shall now consider the set of elements $\{(i,j), j = 1\}$, corresponding to the axis of symmetry $r = 0$. For evaluating their conductivity coefficients, we must start with (5). When the resulting difference equation is multiplied throughout by (17), we get

$$\frac{(h_N+h_S)}{2}\left[\frac{\sigma_{i,j+h_E/2}}{h_E}(v_{i,j+h_E} - v_{i,j}) - \frac{\sigma_{i,j-h_W/2}}{h_W}(v_{i,j} - v_{i,j-h_W})\right] + \left(\frac{h_E+h_W}{2}\right)\left[\frac{\sigma_{i+h_S/2,j}}{h_S}(v_{i+h_S,j} - v_{i,j}) - \frac{\sigma_{i-h_N/2,j}}{h_N}(v_{i,j} - v_{i-h_N,j})\right] + \frac{(h_N+h_S)}{2}\sigma_{i,j}\left[\frac{1}{h_E}(v_{i,j+h_E} - v_{i,j}) - \frac{1}{h_W}(v_{i,j} - v_{i,j-h_W})\right] + \tilde{q}_{i,j} = 0. \tag{35}$$

At this stage we recall that at $r = 0$ condition (12) must also be satisfied. Consequently, (35) requires further modification. In order to do that, we introduce a fictitious column parallel to the vertical axis such that

$$\Delta r(0, 1) = \Delta r(1, 2), \tag{36}$$

$$v_{i,0} = v_{i,2}, \qquad i = 2, 3, \ldots, (i_{max} - 1). \tag{37}$$

Moreover, since we are dealing with a parallel-layer system, we obviously have

$$\sigma_{i,0} = \sigma_{i,2} = \sigma_{i,1}, \qquad i = 2, 3, \ldots, (i_{max} - 1). \tag{38}$$

On account of (38), we can eliminate α_W from (35) by setting $h_W = h_E$. Subsequently, if we again include α_W but set it equal to zero, the set of coefficients for $j = 1$ can be expressed as

$$\left.\begin{aligned} \alpha_E(i, 1) &= 4\sigma_{i,1}\left(\frac{h_N + h_S}{2}\right)/h_E, && (39)\\ \alpha_W(i, 1) &= 0, && (40)\\ \alpha_N(i, 1) &= \sigma_{i-h_N/2,\,1}\, h_E/h_N, && (41)\\ \alpha_S(i, 1) &= \sigma_{i+h_S/2,\,1}\, h_E/h_S. && (42) \end{aligned}\right\} \qquad i = 2, \ldots, (i_{max} - 1)$$

Also, (24) should be replaced by

$$\tilde{q}_{i,1} = q_{i,1}\left(\frac{h_N + h_S}{2}\right)h_E. \tag{43}$$

Relations (39) to (43) do not include the element (1, 1); this element is located at the junction of two Neumann boundaries where conditions (11) and (12) must be satisfied simultaneously. In this case the conductivity coefficients are given by

$$\alpha_E(1, 1) = 8\sigma_{1,1}\left(\frac{h_S}{2}\right)/h_E, \tag{44}$$

$$\alpha_W(1, 1) = 0, \tag{45}$$

$$\alpha_N(1, 1) = 0, \tag{46}$$

$$\alpha_S(1, 1) = 2\sigma_{i+h_S/2,\,1}\, h_E/h_S, \tag{47}$$

$$\tilde{q}_{1,1} = q_{1,1}\, h_E h_S. \tag{48}$$

At the remaining boundaries of the model, viz. *BC* and *CD*, the value of the potential is specified. Therefore, we have considered all the elements where we want to determine the potential field.

Normalization of Current Sources

In most practical problems involving radial symmetry, the sources must be located along the axis of symmetry ($j = 1$). Let an element $(i, 1)$ represent a current source of constant-strength emitting $I_{i,1}$ A. The volume associated with this element is a disc of radius $h_E/2$ and thickness $(h_N + h_S)/2$, but since $j = 1$ is a Neumann boundary, we must consider only one-half of this volume, viz.

$$\tfrac{1}{2}\pi\left(\frac{h_E}{2}\right)^2\left(\frac{h_N + h_S}{2}\right),$$

where $h_E = \Delta r(1, 2)$, $h_N = \Delta z(i - 1, i)$, and $h_S = \Delta z(i, i + 1)$. Therefore, the current density associated with this source can be expressed in the form

$$q_{i,1} = \frac{I_{i,1}}{(\pi/2)(h_E/2)^2\left(\dfrac{h_N + h_S}{2}\right)}. \tag{49}$$

Substitution of (49) into (43) yields

$$\tilde{q}_{i,1} = 8I_{i,1}/(\pi h_E). \tag{50}$$

When the source corresponds to the surface element (1, 1), the volume associated with it represents the limiting case as $h_N \to 0$ (Mufti 1976). Whence

$$q_{1,1} = \frac{I_{1,1}}{(\pi/2)(h_E/2)^2(h_S/2)} \tag{51}$$

and (48) reduces to

$$\tilde{q}_{1,1} = 16I_{1,1}/(\pi h_E). \tag{52}$$

Relation (50) should be used for the investigation of borehole problems such as the numerical evaluation of synthetic electric logs, whereas (52) is suitable for computing surface apparent resistivity curves.

4. Physical Meaning of Conductivity Coefficients

Figs 1 and 2 correspond to a vertical section through a system which is actually in three dimensions. Fig. 3 shows in perspective the element $P(i, j)$ along with its four neighbors E, W, N, and S. The radial distance of P from the vertical axis is denoted by r. In connection with fig. 2, it was mentioned that P stands for the shaded area *abcd*; in three dimensions, it represents a

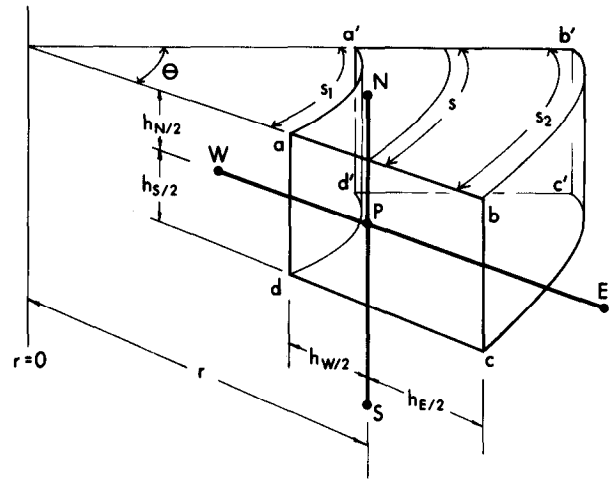

Fig. 3. One of the volume elements constituting a radially symmetric model.

volume element when the area *abcd* is rotated through an angle of 2π around the axis $r = 0$. However, if we normalize the current sources in accordance with (49) and (51), we need to rotate the area *abcd* by such an amount that the length of the arc s swept by P equals unity (fig. 3). In that case, the value of θ measured in radians, equals $1/r$. The lengths of the arcs swept by a and b (or c and d) will be given by

$$s_1 = \frac{1}{r}(r - h_W/2)$$

$$= (1 - h_W/2r), \tag{53}$$

$$s_2 = (1 + h_W/2r). \tag{54}$$

Consequently, the area $aa'dd'$ open to the flow of current from the volume element associated with P to the volume element associated with W can be expressed as

$$\left(1 - \frac{h_W}{2r}\right)\left(\frac{h_N + h_S}{2}\right). \tag{55}$$

Since the distance from P to W is h_W, the block of the medium involved in the passage of current from P to W can be replaced by a conductor of length h_W and cross-sectional area given by (55); its conductance (inverse of resist-

ance) will be given by

$$C_W = \underbrace{\left(\frac{\sigma_P + \sigma_W}{2}\right)}_{\uparrow} \underbrace{\left[\left(1 - \frac{h_W}{2r}\right)\left(\frac{h_N + h_S}{2}\right)\right]}_{\uparrow} \underbrace{\left(\frac{1}{h_W}\right)}_{\uparrow} \tag{56}$$

$$= \begin{matrix}\text{Average} \\ \text{Conductivity}\end{matrix} \times \begin{matrix}\text{Cross-sectional} \\ \text{Area}\end{matrix} \div \text{Length}$$

$$= \sigma_{i,\, j - hw/2}\left(\frac{1}{h_W} - \frac{1}{2r}\right)\left(\frac{h_N + h_S}{2}\right)$$

$$= \alpha_W(i, j), \text{ on account of (20).}$$

Thus, the coefficient $\alpha_W(i, j)$ can be visualized as associated with a conductor whose dimensions are determined by the grid intervals h_N, h_S, and h_W. A similar explanation for the remaining three coefficients α_E, α_N, and α_S is straightforward. Relation (23) will remind the reader of the well-known Kirchhoff's law of currents according to which the sum of currents flowing into the element P must be equal to the total current flowing out of this element. This affords us with the physical explanation of the minus sign preceding the α_P term in (18).

5. Conductivity Coefficients in Terms of Dar Zarrouk Parameters

The element P can also be visualized as representing a portion of a layer indicated by the shaded zone in fig. 2; the thickness of this layer is $(h_N + h_S)/2$. Consequently, (56) can be expressed as

$$\alpha_w(i, j) = \left(\frac{1}{h_W} - \frac{1}{2r}\right) S_W, \tag{57}$$

where

$$S_W = \left(\frac{\sigma_P + \sigma_W}{2}\right)\left(\frac{h_N + h_S}{2}\right). \tag{58}$$

S_W is the unit longitudinal conductance associated with the block of material governing the flow of current across the elements P and W. If we now consider the flow of current across P and E, a relation corresponding to (56) can be expressed as

$$C_E = \frac{\sigma_P + \sigma_E}{2}\left(1 + \frac{h_E}{2r}\right)\left(\frac{h_N + h_S}{2}\right)\left(\frac{1}{h_E}\right). \tag{59}$$

This leads to:

$$\alpha_E(i, j) = \left(\frac{1}{h_E} + \frac{1}{2r}\right) S_E, \tag{60}$$

where

$$S_E = \left(\frac{\sigma_P + \sigma_E}{2}\right)\left(\frac{h_N + h_S}{2}\right).$$

We shall now consider the remaining two coefficients $\alpha_N(i, j)$ and $\alpha_S(i, j)$. Referring to fig. 3, since the length of the arc s is unity, the area open to the flow of current from P to N will be given by

$$(h_E + h_W)/2.$$

Therefore, the block of material involved in this case can be replaced by a conductor whose conductance is given by

$$C_N(i, j) = \left(\frac{\sigma_P + \sigma_N}{2}\right)\left(\frac{h_E + h_W}{2}\right)\frac{1}{h_N} \tag{61}$$

$$= \alpha_N(i, j), \text{ on account of (21).}$$

This leads to the relation

$$\alpha_N(i, j) = \left(\frac{h_E + h_W}{2}\right)/T_N, \tag{62}$$

where

$$T_N = h_N/\left(\frac{\sigma_P + \sigma_N}{2}\right).$$

T_N is the unit transverse resistance involved in the passage of current across P and N. Similarly, we obtain the relations

$$\alpha_S(i, j) = \left(\frac{h_E + h_W}{2}\right)/T_S, \tag{63}$$

$$T_S = h_S/\left(\frac{\sigma_P + \sigma_N}{2}\right).$$

Note that, when we are dealing with a system of parallel layers, each representing a uniform and isotropic medium $S_E = S_W$, but, in general, $T_N \neq T_S$.

The above-mentioned treatment implies that resistivity may vary at most from one element to the next, but not in between. Thus if we are considering a

large number of thin parallel layers, each layer must be assigned at least one horizontal grid line, otherwise its presence will not influence the results. We are now going to generalize our method of computing the conductivity coefficients such that all layers can be properly taken into account even when we do not assign a set of grid locations to each individual layer constituting the model.

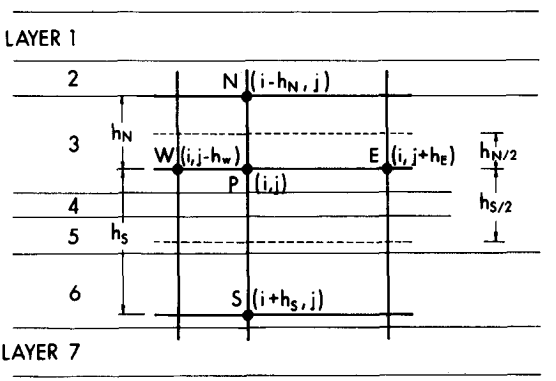

Fig. 4. Vertical section of a layered medium superimposed by a logarithmically expanding grid system.

Fig. 4 shows a vertical section through a sequence of parallel layers, each one of which may be assigned arbitrary values of resistivity and thickness. This system is superimposed by a number of grid lines similar to those shown in fig. 1. The boundary of the area associated with the element P is indicated by broken lines. As mentioned before, this area is a portion of a layered medium of thickness $(h_N + h_S)/2$. To be more specific, it consists of three different layers, viz. layers 3, 4, and 5. Of course, we must consider only portions of layers 3 and 5 which fall within the thickness range $i - h_N/2$ to $i + h_S/2$. Consequently, the coefficients $\alpha_E(i, j)$ and $\alpha_W(i, j)$ will now be determined by the longitudinal conductance of all the three layers involved. Similarly, in computing $\alpha_N(i, j)$, we must consider the transverse resistance due to all the layers over the thickness range i to $i - h_N$. A similar argument applies to the coefficient $\alpha_S(i, j)$, for which the range of thickness will be from i to $i + h_S$. At this stage we are ready to generalize the procedure for expressing the conductivity coefficients in terms of the longitudinal conductance and transverse resistance, usually known as the Dar Zarrouk parameters. Let the number of layers traversed from the depth $i - h_N$ to i be denoted by r, from depth i to $i + h_S$ by s, from depth $i - h_N/2$ to i by p and from depth i to $i + h_S/2$ by q. We shall use this notation to define the conductivity coefficients for the various sets of elements.

$i = 2, 3, \ldots, (i_{max} - 1); \qquad j = 2, 3, \ldots, (j_{max} - 1)$:

$$\alpha_E(i, j) = \left(\frac{1}{h_E} + \frac{1}{2r}\right) \sum_{k=1}^{p+q} h_k \sigma_k, \tag{64}$$

$$\alpha_W(i, j) = \left(\frac{1}{h_W} - \frac{1}{2r}\right) \sum_{k=1}^{p+q} h_k \sigma_k, \tag{65}$$

$$\alpha_N(i, j) = \left(\frac{h_E + h_W}{2}\right) \sum_{k=1}^{r} h_k/\sigma_k, \tag{66}$$

$$\alpha_S(i, j) = \left(\frac{h_E + h_W}{2}\right) \sum_{k=1}^{s} h_k/\sigma_k. \tag{67}$$

$i = 1; j = 2, 3, \ldots, (j_{max} - 1)$:

$$\alpha_E(1, j) = 2\left(\frac{1}{h_E} + \frac{1}{h_r}\right) \sum_{k=1}^{q} h_k \sigma_k, \tag{68}$$

$$\alpha_W(1, j) = 2\left(\frac{1}{h_W} - \frac{1}{2r}\right) \sum_{k=1}^{q} h_k \sigma_k, \tag{69}$$

$$\alpha_N(1, j) = 0, \tag{70}$$

$$\alpha_S(1, j) = (h_E + h_W)/\left(\sum_{k=1}^{s} h_k/\sigma_k\right). \tag{71}$$

$j = 1; i = 2, 3, \ldots, (i_{max} - 1)$:

$$\alpha_E(i, 1) = \frac{4}{h_E} \sum_{k=1}^{p+q} h_k \sigma_k, \tag{72}$$

$$\alpha_W(i, 1) = 0, \tag{73}$$

$$\alpha_N(i, 1) = h_E/\left(\sum_{k=1}^{r} h_k/\sigma_k\right), \tag{74}$$

$$\alpha_S(i, 1) = h_E/\left(\sum_{k=1}^{s} h_k/\sigma_k\right), \tag{75}$$

$i = 1; j = 1$:

$$\alpha_E(1, 1) = \frac{8}{h_E} \sum_{k=1}^{q} h_k \sigma_k, \tag{76}$$

$$\alpha_W(1, 1) = 0, \tag{77}$$

$$\alpha_N(1, 1) = 0, \tag{78}$$

$$\alpha_S(1, 1) = 2h_E/\left(\sum_{k=1}^{S} h_k/\sigma_k\right). \tag{79}$$

For any given set of grid spacings, relations (64) to (79) can be used for computing the potential field for all possible layered media. We shall now devise an optimum discretization scheme.

6. Evaluation of Apparent Resistivity Curves

From now on, our primary objective is to compute apparent resistivity curves for the Schlumberger configuration. It may be pointed out that for parallel layers the potential field due to a current dipole can be computed by considering only one current source located at the origin in the simulation model. Let us discretize the finite-difference model along the radial direction in such a manner that the distances of the successive elements increase by a constant factor a. Thus, if the element P is at a distance r_P from the source, the corresponding distances of W and E will be r_P/a and $r_P a$, respectively

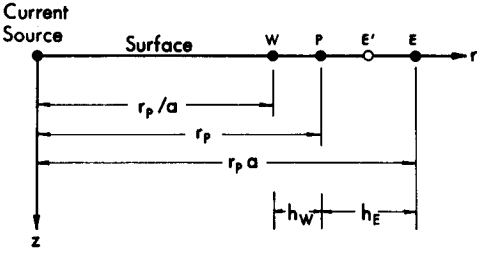

Fig. 5. A resistivity model in which the distance of vertical grid lines from the source expands by a factor of a.

(fig. 5). In that case the apparent resistivity for the Schlumberger configuration is given by (Koefoed 1968, p. 10)

$$\rho_a = -\frac{\pi r_p^2}{I}\left(\frac{dv}{dr}\right)_{r=r_p}, \tag{80}$$

where (dv/dr) with $r = r_P$ represents the derivative of the potential at the element P. Now let the values of the potential computed from the model at W, P, and E be denoted by v_W, v_P, and v_E. Also, since the variation of the field between any two consecutive elements in a finite-difference model is linear, the potential at a fictitious element E' located on the right side of P at distance h_W from it can be obtained by interpolation; it can be expressed as

$$v_{E'} = v_P + (v_E - v_P)\frac{h_W}{h_E}.$$

Therefore,

$$\left(\frac{dv}{dr}\right)_{r=r_P} = \frac{1}{2h_W}(v_{E'} - v_W) = \tfrac{1}{2}[(v_P - v_W)/h_W + (v_E - v_P)/h_E]. \quad (81)$$

For each element, the intervals h_E and h_W depends on the choice of a. Actual field experience shows that no useful information can be gathered (except in very noisy conditions) if we expand the current electrodes more slowly than by a factor of $\sqrt{2}$ in successive steps (Kunetz 1966, p. 84). Consequently, for a theoretical model set up in a noise-free environment, $a = \sqrt{2}$ should provide a sufficiently fine grid system. However, since (81) involves some interpolation, let us choose $a = 2^{1/3}$. Thus, if $j = 1$, $(r = 0)$ corresponds to the location of the source, the radial distance of the grid lines $j = 2, 3, \ldots$ from the source will be $1, 2^{1/3}, 2, 2^{4/3}, \ldots$. In deciding about the horizontal grid intervals, we keep in view the recent studies carried out by Marsden (1973) and Flathe (1974). They point out that our chances of detecting a layer in a horizontally stratified earth are greatly reduced if (1) the ratio of its resistivity to that of the neighbouring layers is less than 1 : 3 and (2) its thickness is less than that of the total overburden. The second rule implies that the distance of successive horizontal grid lines from the surface of the ground ($i = 1$) may increase in a geometric progression with $a = 2$. As a compromise between these two empirical rules, let us choose $a = \sqrt{2}$ so that $i = 2, 3, 4, \ldots$ is at depths $1, 2^{1/2}, 2, 2^{3/2}, \ldots$. Those layers which turn out to be too thin for this sampling scheme still influence the results provided the longitudinal conductance or transverse resistance associated with them significantly modifies the conductivity coefficients of the model.

Each element of the finite-difference model with unknown potential gives rise to an equation, and the evaluation of the potential field requires the solution of a system of equations by inverting a matrix. Further details of setting up the matrix and handling special problems arising at the boundaries of the model are discussed in detail by Mufti (1976). It may be added, however, that the discretization scheme presented above results in a reasonably small matrix which can be inverted more efficiently by direct methods of handling sparse matrices than by using a relaxation algorithm. One of the most efficient methods of inverting the type of matrices arising in resistivity modeling is known as the alternate diagonal ordering scheme; it was first reported by Price and Coats (1974). A comprehensive software package suitable for inverting a variety of sparse matrices is developed by Eisenstat, Gursky, Schultz and Sherman (1977).

Now we present the numerical examples computed by using the above-mentioned scheme with $i_{max} = 24$ and $j_{max} = 35$. The following parameters

were used

	Resistivity Ratios	*Thickness Ratios*
Example 1 (three layer case)	1 : 10 : 2.5	1 : 5 : ∞
Example 2 (four layer case)	1 : 5 : 0.4 : 1	1 : 1 : 10 : ∞

The results are shown in figs 6 and 7. For the sake of comparison, the corresponding analytical data obtained from the tables published by Orellana and Mooney (1966) are also plotted on the same scale. The two sets of

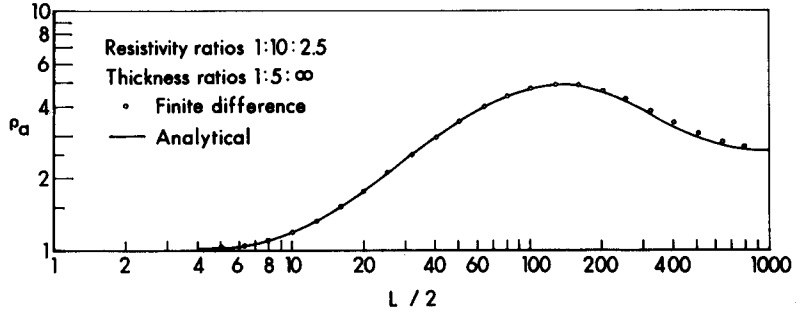

Fig. 6. Apparent resistivity curve for a three-layer medium obtained by finite-difference modeling.

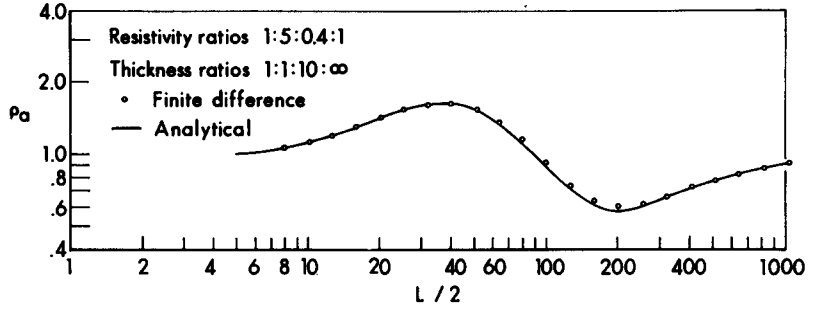

Fig. 7. Apparent resistivity curve for a four-layer medium obtained by finite-difference modeling.

data are practically identical except for a slight departure in fig. 7 over the depth range of 80–200. We should not readily conclude that the analytical data are more accurate. As a matter of fact, Orellana and Mooney do not provide any estimates of accuracy of their results, whereas in the case of finite-difference data such estimates are hard to obtain.

Concluding Remarks

Numerical evaluation of apparent resistivity curves by analytical means is not an easy problem. This is true even for the relatively simple geologically realistic models consisting of parallel layers. However, the same problem when properly formulated within the framework of a finite-difference technique becomes intrinsically simple. It is treated by us in cylindrical coordinates so that the potential field due to a point source can be conveniently computed.

The procedure adopted for discretizing the medium is a significant departure from the conventional style of setting up finite-difference models. Most often, one uses a uniform but sufficiently dense grid spacing so that the essentially non-uniform potential field which varies particularly rapidly in the vicinity of the source(s) can be appropriately sampled. This results in very large models. On the other hand, the use of non-uniform grid spacing depends on the geology of the model so that each individual layer may be taken into account. The latter scheme usually results in somewhat smaller models but yields less accurate results and necessitates a new grid spacing for every little change in the geology of the model. The procedure introduced by us involves the use of a system of horizontal and vertical grid lines whose distance increases logarithmically from the source. It was motivated by the fact that one cannot push the limits of resolution inherent in the resistivity method simply by sampling the earth more densely. Of course, one must also keep in mind that failure to consider a thin but anomalously resistive or conductive layer at depth will lead to erroneous results. This problem was overcome by defining the conductivity coefficients associated with the various layered blocks in terms of Dar Zarrouk parameters. Consequently, the same discretization scheme can be used for all possible resistivity and thickness ratios. The biggest single advantage appears to lie in the computational efficiency. The potential field is computed by inverting a surprisingly small matrix with very modest requirements both in terms of computer time and storage memory. Unlike the analytical model, the finite-difference model is almost immune to geologic complexity. When the structure under investigation consists of only a few layers, the efficiency of the finite-difference model is comparable to that of the corresponding analytical model. However, when we are dealing with complicated systems consisting of a large number of layers which arise, for example, in the iterative solution of inverse problems or in the computation of synthetic electric logs, the finite-difference model turns out to be more efficient than the analytical model.

ACKNOWLEDGMENTS

The author is indebted to Dr S. N. Domenico and Dr W. G. Clement for many valuable suggestions and criticisms. The manuscript was reviewed by Dr Barkev Bakamjian. Permission from Amoco Production Company to publish this work is greatly appreciated.

REFERENCES

ANONYMOUS—Uses. Nauchn. Issled. Inst. Geofiz. 1963a Al'bom Paletok Electricheskogo Zondirovanya dlya Trekhsloinykh Gorizontal'no-Odnorodnykh Razrezov (master curves), Gosgeoltekhizdat, Moskva.

ANONYMOUS—Uses. Nauchn. Issled. Inst. Geofiz. 1963b, Al'bom Paletok, Elektricheskogo Zondirovanya dlya Chetirekhsloinykh Gorizontal'no-Odnorodnykh Razrezov (master curves), Moskva.

ARGELO S.M. 1967, Two computer programs for the calculation of standard graphs for resistivity prospecting, Geophysical Prospecting 15, 71–91.

BHATTACHARYA P.K. and PATRA H.P. 1968, Direct geoelectric sounding, Elsevier Publishing Co., Amsterdam.

BORM G. 1972, Zur Theorie eines Netzwerkmodelles für geoelektrische Analogmessungen, Zeitschrift für Geophysik 38, 791–810.

BORM G. 1973, Solutions of boundary value problems of multilayer analog of geoelectrics and hydrology, Zeitschrift für Geophysik 39, 41–78.

COMPAGNIE GÉNÉRALE DE GÉOPHYSIQUE, 1963. Master curves for electrical sounding, 2nd Ed., European Assoc. Exploration Geophysicists, The Hague.

DAM J.C. VAN 1965, A simple method of the calculation of standard graphs to be used in geolectric prospecting, Geophysical Prospecting 13, 37–65.

DEPPERMANN K. 1973, An interpretation system for geoelectric sounding graphs, Geophysical Prospecting 21, 424–463.

EISENSTAT S.C. GURSKY M.C. SCHULTZ M.H. and SHERMAN A.H. 1977, Yale sparse matrix package, Research Reports No. 112 and 114, Dep. of Computer Science, Yale University, Yale, Connecticut.

EUROPEAN ASSOC. EXPLORATION GEOPHYSICISTS, 1969, Standard Graphs for resistivity prospecting, E.A.E.G., The Hague.

FLATHE H. 1955, A practical method of calculating geoelectrical model graphs for horizontally stratified media, Geophysical Prospecting 3, 268–294.

FLATHE H. 1974, Comment on "The automatic fitting of a resistivity sounding by geometrical progression of depths," Geophysical Prospecting 22, 176–180.

GHOSH D.P. 1971a, The application of linear filter theory to the direct interpretation of geoelectrical resistivity sounding measurements, Geophysical Prospecting 19, 192–217.

GHOSH D.P. 1971b, Inverse filter coefficients for the computation of apparent resistivity standard curves for a horizontally stratified earth, Geophysical Prospecting 19, 769–775.

HUMMEL J.N. 1932, Theoretical study of apparent resistivity in surface potential methods, Geoph. Vol. A.I.M.E.

KOEFOED O. 1968, The application of the kernel function in interpreting geoelectrical resistivity measurements, Gebrüder Borntraeger, Berlin.

KUNETZ G. 1966. Principles of direct current resistivity prospecting, Gebrüder Borntraeger, Berlin.

MAILLET R. 1947, The fundamental equations of electrical prospecting, Geophysics 12, 529–556.

MARSDEN D. 1973, The automatic fitting of a resistivity sounding by geometric progression of depths, Geophysical Prospecting 21, 266–280.

MOONEY H.M. ORELLANA E. PICKETT H. and TORNHEIM L. 1966, A resistivity computation method for layered earth models, Geophysics 31, 192–203.

MOONEY H.M. and WETZEL W.W. 1956, The potential about a point electrode and apparent resistivity curves for a two-, three-, and four-layer earth, Minneapolis, Univ. Minnesota.

MUFTI I.R. 1976, Finite difference resistivity modeling for arbitrarily shaped two dimensional structures, Geophysics 41, 62–78.

ORELLANA E. and MOONEY H.M. 1966, Master tables and curves for vertical electrical sounding over layered structures, Intersciencia, Madrid.

PRICE H.S. and COATS K.H. 1974, Direct methods in reservoir simulation, Soc. of Pet. Engrs. Journ., 14, 295–308.

STEFANESCO S.S., SCHLUMBERGER C. and SCHLUMBERGER M. 1930, Sur la distribution électrique potentielle autour d'une prise de terre ponctuelle dans un terrain à couchés horizontales homogénes et isotropes, Journ. Physique et Radium, Ser. 7, v. 1, 132–141.

TAGG G.F. 1932, Interpretation of resistivity measurements Am. Inst. Mining Metall. Engineers Tech. Pub. 477, 13 p. 1934, Trans. 110, 135–147.

YOUNG D. 1962, The numerical solution of elliptic and parabolic partial differential equations, *in* Survey of numerical analysis, Edited by J. Todd, 380–438, McGraw-Hill Book Co., Inc., New York.